The following publication H. Bao, W. Jin, Y. Miao and H. L. Ho, "Laser-Induced Dispersion With Stimulated Raman Scattering in Gas-Filled Optical Fiber," in Journal of Lightwave Technology, vol. 37, no. 9, pp. 2120-2125, 1 May, 2019 is available at https://doi.org/10.1109/JLT.2019.2898463.

Laser induced dispersion with stimulated Raman scattering in gas-filled optical fiber

Haihong Bao, Wei Jin, Senior Member, IEEE, Yinping Miao and Hoi Lut Ho

***Abstract*—Laser induced dispersion provides an all-optical means for dynamically controlling light propagation. Previous works on dispersion control with a laser beam make use of Kerr non-linearity, electromagnetic induced transparency and stimulated Brillouin scattering in optical fibers. Here we report, for the first time to our knowledge, optically controllable dispersion with stimulated Raman scattering in a gas-filled hollow-core optical fiber and show that flexible dispersion tuning can be achieved by varying optical pump power and wavelength as well as gas concentration and pressure in the hollow-core. As an example of application, we demonstrated the use of such laser induced dispersion for high sensitivity hydrogen detection and achieved a normalized detection limit of 17.4 ppm/(m·W) with dynamic range over 4 orders of magnitude.**

***Index Terms*—gas sensor, optical fiber sensor, Raman scattering, Raman induced dispersion**

I. Introduction

LIGHT dispersion in optical fibers has numerous applications in optical sensing, communication and signal processing. Traditionally, dispersion control is achieved via fiber geometry and material composition. However, dispersion can also be actively manipulated with a separate laser beam through nonlinear light-matter interaction such as cross-phase modulation (XMP) [1], [2], electromagnetically induced transparency (EIT) [3]–[5] and stimulated Brillouin scattering (SBS) [6]–[9]. Such laser induced dispersions have been exploited for photonic sensors [10], switches and tunable optical delay lines [11]. XMP modifies the refractive index (RI) of the waveguide material, and the interplay of RI modulation and waveguide structure allows dispersion control of a guided mode. However, the degree of control is limited due to the weak dependence of RI modulation on wavelength. EIT and SBS induce much sharper dispersion changes near narrow optical resonances. However, EIT works around a fixed wavelength dictated by gas molecular absorptions and typically operating under low gas pressure [4]. SBS resonances can be located at a desired wavelength by tuning the pump wavelength, but SBS in conventional solid optical fibers are primarily determined by the core material (i.e., doped silica) and the resonance linewidth could not be tuned easily [12].

Stimulated Raman scattering (SRS) results from nonlinear interaction between two laser beams (pump and Stokes) and a Raman-active medium. SRS in solid optical fibers has been used for optical signal amplification [13] and distributed optical fiber temperature sensing [14], and SRS in gas- or liquid-filled hollow-core photonic crystal fibers (HC-PCFs) has been studied for trace chemical detection [15], [16]. However, these reported works exploit the gain feature of SRS. In fact, SRS simultaneously induces RI changes near the Stokes wavelength, resulting in dispersion change around the Raman resonances [17]. The Raman resonances in gases are typically very narrow, from sub to a few GHz, resulting sharp dispersion change around the Raman resonances. The position, magnitude and linewidth of the Raman resonance and hence the dispersion change can, in principle, be dynamically tuned by varying the wavelength and power level of the pump source as well as the pressure, composition and concentration of gases, providing a highly flexible means of controlling light dispersion. However, there seems no report on this to our knowledge.

In this article, we report laser induced dispersion with SRS in a gas-filled HC-PCF. The theory of SRS induced dispersion is outlined and the benefits of using HC-PCF are revealed. The tuning of SRS-induced dispersion by varying the hydrogen-nitrogen mixing ratio and pump power level is then demonstrated. As a potential application, hydrogen detection down to ppm level is realized.

II. Theory

A pump laser beam (ω_{pump}) and a weaker probe laser beam (ω_{probe}) are co-propagating in a gas-filled HC-PCF, as illustrated in Fig. 1(a). When the frequency difference between the two laser beams is in the vicinity of a molecular Raman transition (W_0) of gases in the hollow-core (Fig. 1(b)), i.e. $\omega_{pump}-\omega_{probe}\approx\omega_{pump}-\omega_{Stokes}=\omega_0$, SRS induces a complex RI modulation of the gas material [18]:

$$\Delta n(W_{probe}) = -i\frac{cg_0 I_{pump}}{2W_{probe}\left\{1-i2\left[W_0-\left(W_{pump}-W_{probe}\right)\right]/\Gamma_R\right\}} \quad (1)$$

where $\Gamma_R/2\pi$ is the linewidth of the Raman resonance, c is light speed, g_0 is the peak gain coefficient that is proportional

Manuscript received XXX, 2018; revised XXX, 2018; accepted XXX, 2018. Date of publication XXX 2018; date of current version XXX, 2018. The research work was supported by Hong Kong SAR government through GRF grant PolyU 152210/18E, Natural Science Foundation of China through grant 61535004, and the Hong Kong Polytechnic University through Grants 1-ZVG4 and 4-BCD1. (Corresponding author: Wei Jin.) The authors are with the Department of Electrical Engineering, The Hong Kong Polytechnic University, Hung Hom, Kowloon, Hong Kong, and also with The HongKong Polytechnic University Shenzhen Research Institute, Shenzhen, China (e-mail: edward.bao@connect.polyu.hk; eewjin@polyu.edu.hk; kikosi@126.com; eehlho@polyu.edu.hk).

to gas concentration (C) and I_{pump} is the pump light intensity. The interaction between the pump, probe and gas molecules results in energy transfer from pump to probe as well as sharp RI (dispersion) change around the Stokes frequency, as illustrated in Fig. 1(c). The gain experienced by the probe beam is related to the imaginary part of $\Delta n(\omega_{probe})$, while the dispersion is proportional to the real part of $\Delta n(\omega_{probe})$. The dramatic change in dispersion effectively modifies the group RI of the probe beam, which is also illustrated in Fig. 1(c). Raman scattering in gases is extremely weak. However, the use of a HC-PCF enables tighter light field confinement, nearly perfect overlap of gas sample with light fields and long length for light-gas interaction [15], [19]–[21], which greatly enhances the SRS. The induced RI change may be detected by measurement of the accumulated phase of the probe beam over a length of L. The accumulated phase change can be expressed as [22]:

$$\Delta\phi(\delta) = \frac{2\pi}{\lambda_{probe}} \mathrm{Re}\left[\Delta n(\omega_{probe})\right] L = \left(\frac{\delta}{1+\delta^2}\right)\Delta\phi_0, \qquad (2)$$

Where $\delta = 2\left[\omega_0 - \left(\omega_{pump} - \omega_{probe}\right)\right]/\Gamma_R$ is the linewidth-normalized frequency detuning parameter and $\Delta\phi_0 = G/2$ is the peak phase change which is related to the accumulated gain $G = g_0 I_{pump} L$ at the Raman resonance.

The laser induced dispersion with SRS in a gas-filled optical fiber has great flexibility. Firstly, the spectral location of the induced dispersion, being determined by $\omega_{Stokes} = \omega_{pump} - \omega_0$, can be tuned by varying the pump wavelength. The possibility of exciting multiple Raman transitions simultaneously in a HC-PCF filled with single or multiple gases with different concentration and by use of single or multiple pump sources would enable dispersion control at multiple spectral locations over a wide wavelength range. Secondly, the Raman linewidth as well as the peak gain coefficient g_0 are gas-pressure dependent, which provides another degree of freedom to control the magnitude and spectral range of the induced dispersion. The pump light intensity as well as the length of gas-filled fiber can also be adjusted to control the magnitude of dispersion and the accumulated phase change.

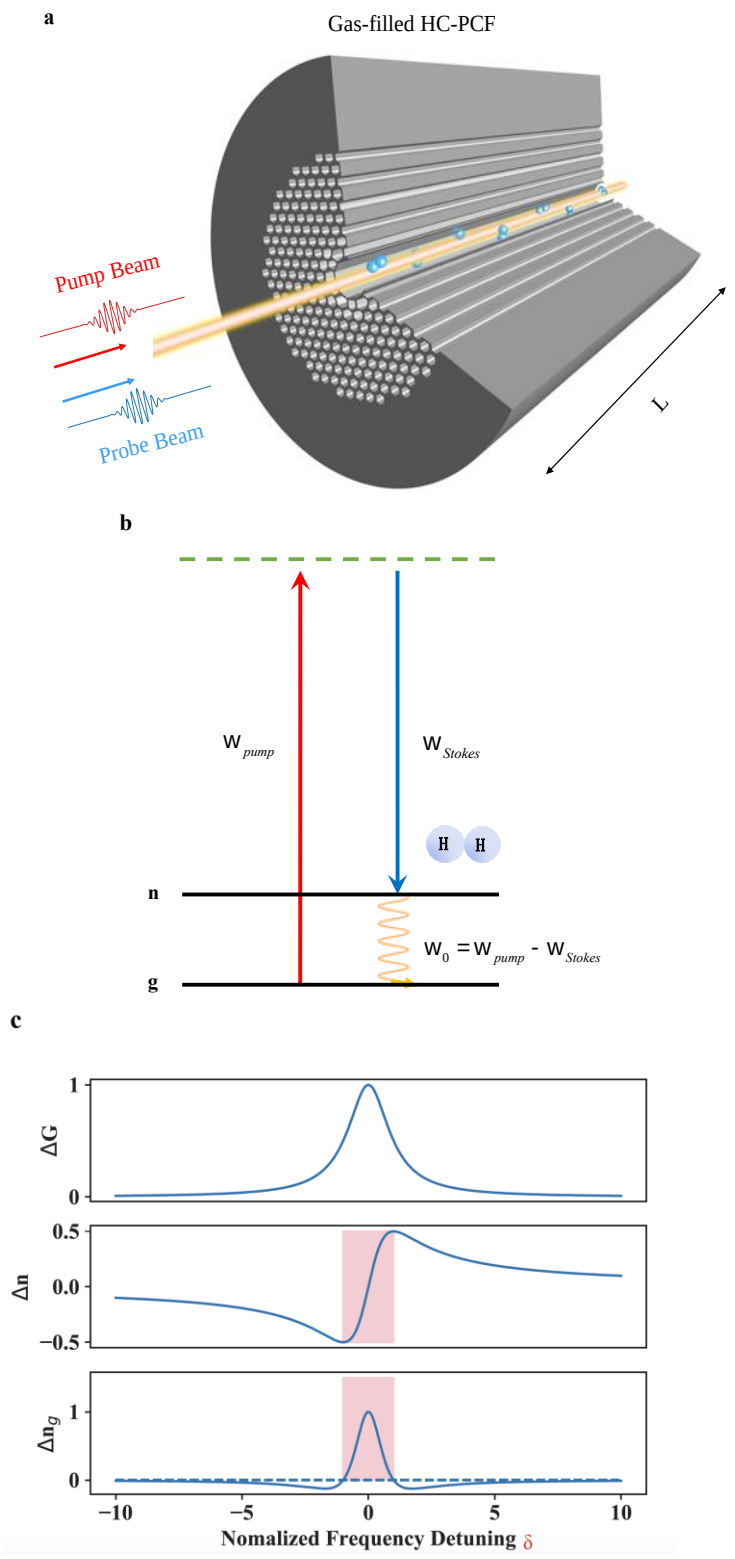

Fig. 1. Theoretical description. a, A pump beam (ω_{pump}) and a probe beam (ω_{probe}) co-propagate in a HC-PCF. b, Energy level diagram describing the SRS process. g is the ground state; n is the rotational state; the dotted line is the intermediate state. **c,** The probe light experiences Raman gain (ΔG), RI change (Δn) and group RI change (Δn_g) at the vicinity of Stokes frequency ω_{Stokes}. The shaded pink area indicates the linewidth of Raman resonance, which corresponds to $-1 \le \delta \le 1$.

III. Experiments and Results

A. Dispersion Measurement

We experimentally measured the SRS-induced dispersion around the $S_0(0)$ rotational Raman transition of hydrogen with a Raman shift ω_0=354.36 cm^{-1} [23]. The experimental setup is depicted in Fig. 2. The HC-PCF and single mode fiber (SMF) are inter-connected through ceramic ferrules. Hydrogen and nitrogen mixtures of different ratio is pressurized into a 7-m-long HC-1550-06 fiber (NKP Photonics) through the gap between SMF and HC-PCF. The pump beam is from a distributed feedback (DFB) semiconductor laser with nominal wavelength ~1532.1 nm. The pump power is boosted with an Er-doped fiber amplifier (EDFA) and delivered to the gas-filled HC-PCF.

The induced dispersion is related to the accumulated phase change of the probe light via equation (2), which can be measured by using a Sagnac [24] or Mach-Zehnder interferometer (MZI) [25] powered by a probe laser tuned to the Stokes wavelength. Here we used an all-fiber MZI powered by an external cavity diode laser (ECDL) with its wavelength fixed to 1620.055 nm. To ensure dispersion measurement with high signal-to-noise ratio (SNR), we employed a technique similar to that used in wavelength modulation spectroscopy [25]: the pump wavelength is sinusoidally modulated at f = 51 kHz and at the same time slowly scanned so that the wavelength difference between the pump and probe beams is tuned across the $S_0(0)$ transition of hydrogen. This modulates the phase of the probe beam, which includes harmonic components of the modulation frequency. The phase modulation is then converted to intensity modulation by the MZI stabilized at quadrature with a servo-loop [25]. The second harmonic ($2f$) of the MZI output, which is linearly proportional to the $2f$ component of the probe light phase modulation, is lock-in detected and used as the system output. The depth of pump wavelength modulation is set to 2.84 to maximize the $2f$ output signal [26] (see appendix.). Balanced detection using the two outputs from the MZI ensures that the small induced Raman gain would not affect the dispersion measurement [27].

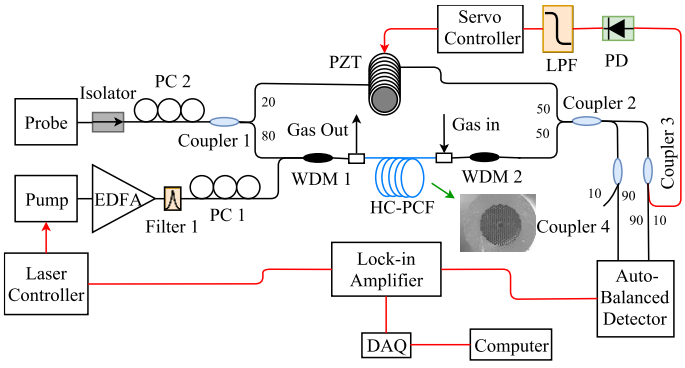

Fig. 2. Experimental setup for laser induced dispersion measurement. LPF: low-pass-filter; DAQ: data acquisition; PC: polarization controller; EDFA: erbium doped fiber amplifier; PZT, piezoelectric transducer for phase compensation. Inset: scanning electron microscopy of the HC-PCF (HC-1550-06 fiber with core diameter of ~11 μm). Filter 1 is used to filter out the amplified spontaneous emission noise of EDFA. WDM 1&2: 1620nm/1530nm wavelength-division multiplexer. WDM 1 is used to combine the pump and probe beams and WDM 2 is used to filter out the pump.

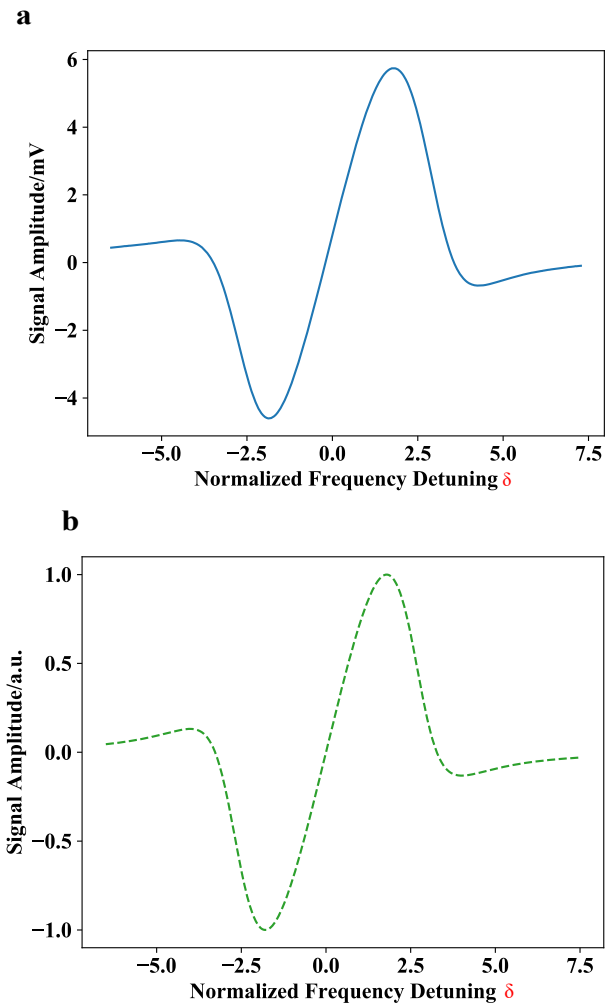

Fig. 3. a, Measured and b, calculated $2f$ signal due to laser induced dispersion near the $S_0(0)$ transition of hydrogen. Pure hydrogen is filled into the HC-PCF with a pressure of 3.5 bar. The modulation depth is 2.84.

Fig. 3(a) shows the measured $2f$ signal for pure hydrogen with the gas pressure of 3.5 bar inside the hollow-core with a pump power of ~100 mW delivered to the HC-PCF, corresponding to a peak pump intensity of 0.314 MW/cm^2 at the center of the hollow-core. For comparison, the $2f$ signal is numerically calculated based on the formulations in [26] and shown in Fig. 3 (b), agreeing well with the measured result.

The SRS-induced dispersion can be actively controlled by varying the concentration of gases in the hollow-core. Fig. 4(a) shows the measured $2f$ signal around the Raman resonance with pump power of ~100 mW for different hydrogen concentration of 4, 20 and 100% at 3.5 bar. The peak-to-peak value of the $2f$ signal, which is proportional to dispersion change, has a linear relationship with gas concentration as shown in Fig. 4(b). The magnitude of dispersion change can also be adjusted by varying pump laser power in the hollow-core. Fig. 4(c) shows $2f$ signal for a HC-PCF filled with 20% hydrogen balanced with nitrogen for four different pump power levels. Fig. 4(d) shows that the $2f$ signal has a good linear relationship with pump power, agreeing with the prediction from equation (2). Such a SRS-induced dispersion can be useful for a range of applications such as optical pulse walk-off cancellation [28] and precision gas spectroscopy.

B. Gas Detection

Hydrogen detection is important for energy and safety applications, but the popular techniques based on laser absorption spectroscopy cannot be used since hydrogen has no absorption in the visible and infrared wavelength regions. Previous detection of hydrogen is based on hydrogen sensitive coatings and electrochemical materials, which have limitations in selectivity, sensitivity, dynamic range and repeatability [29], [30]. Raman spectroscopy can detect Raman-active gases that do not necessarily have absorption lines, providing effective means for hydrogen detection with high selectivity [31]. Under high pressure (i.e., 20 bars) condition, gas detection down to several ppm has been achieved using a meter-long HC-PCF (HC-580-02 from NKT Photonics) with collimating optics, 2W pump laser at 532 nm and Roper Scientific spectrometer (Model Acton 2556) equipped with liquid-nitrogen-cooled CCD [32]. However, the system is bulky and inconvenient for practical applications. Recently demonstrated all-fiber hydrogen gas sensors based on stimulated Raman gain spectroscopy (SRGS) have the capability for remote detection and are flexible for practical applications. However, the limit-of-detection (LOD) is ~140 ppm for 1 second integration time with 15-m-long HC-PCF, limited by the intensity fluctuation received at the photodetector [15].

As discussed in Section III-*A*, the SRS-induced dispersion is proportional to gas concentration and can therefore be exploited for spectroscopic gas detection. It has been shown by others that the molecular dispersion-based laser absorption spectroscopy sensors have better immunity to photo-detected intensity fluctuation as well as a larger dynamic range over the intensity-based measurement [33]. The interferometric detection of SRS-induced dispersion, which has not been reported previously, is expected to provide the same advantages and with additional benefit: the SRS-induced dispersion can be modulated by modulating the pump beam, which allows the use of a fixed probe with a stabilized fiber interferometer to minimize noise and fluctuations resulting from the modulation of the probe beam. We name this technology as stimulated Raman dispersion spectroscopy (SRDS).

To evaluate the potential of the technique for high sensitivity hydrogen detection, we measured the system noise level by tuning the pump wavelength away from the Raman resonance to 1531.956 nm. The standard deviation of noise for the four different pump power levels are shown in Fig. 4 (d) as the red diamonds. For a pump power of ~ 98.4 mW, the peak-to-peak 2*f* output signal for 20% hydrogen is ~2.2 mV and the standard deviation of noise is 0.273 μV for 1s lock-in time constant, corresponding to the detection bandwidth of 0.094 Hz. This gives a SNR of 8059. The detection limit in terms of noise equivalent concentration (NEC) for a SNR of unity is then estimated to be 25 ppm, or a normalized NEC (NNEC) of ~17.4 ppm/(m·W). The dynamic range of the system is estimated to be more than 4 orders of magnitude from the minimum detection level to 100% hydrogen. The largest phase modulation for 100% hydrogen is estimated to be ~10^{-3} rad, well within the linear region around the quadrature point of the MZI. From Fig. 4(d), the 2*f* signal increases approximately linearly with the pump power while the noise level remained relatively unchanged, indicating further improvement of detection limit is possible by simply increasing the pump power level.

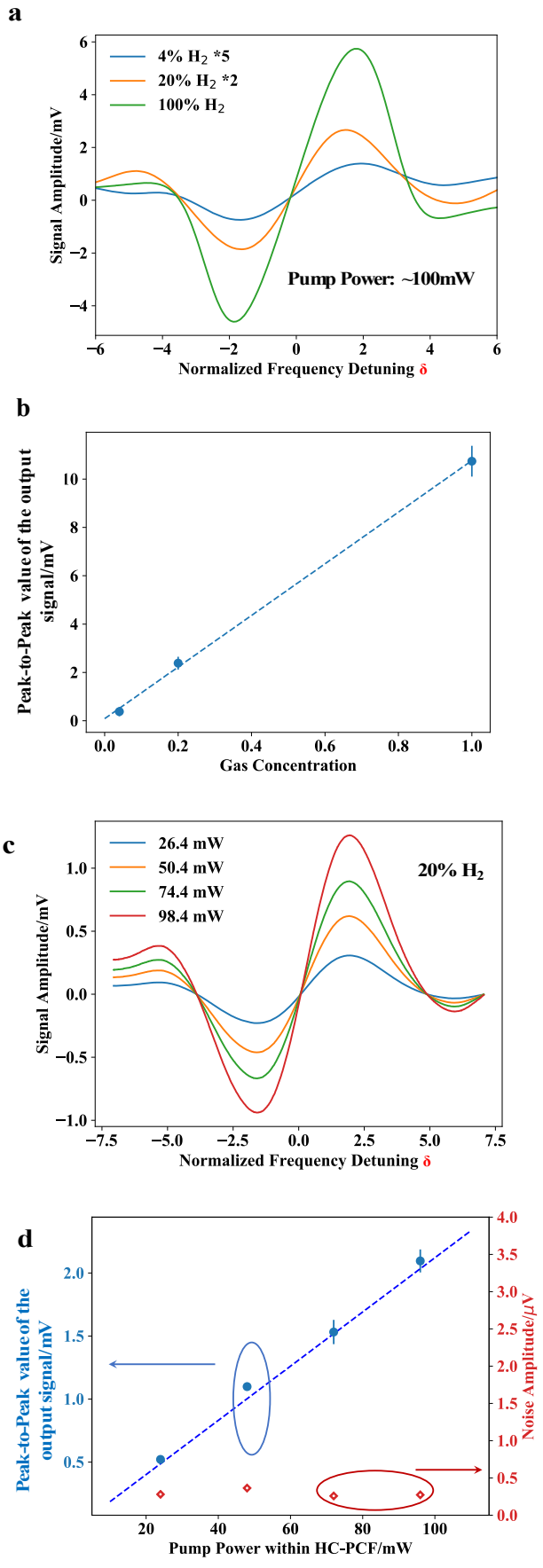

Fig. 4. Experimental results of actively controlling laser induced dispersion with SRS. a and b are results of controlling SRS-induced dispersion by changing hydrogen concentration. a, Measured 2*f* output signal when pump beam is scanned across the $S_0(0)$ Raman transition of hydrogen of different concentration. The 2*f* output signals for 4% and 20% hydrogen are scaled up 5 and 2 times respectively for better presentation; b, The peak-to-peak value of 2*f* output signal as function of gas concentration. Error bars show the standard deviation from 10 measurements and their magnitudes are scaled up 10 times for better clarity. c and d are results of controlling SRS-induced dispersion by changing pump power with 20% hydrogen; c, The 2*f* output signal when pump wavelength is tuned across Raman transition line with different power levels and 20% hydrogen; d, Peak-to-peak value of 2*f* output signal for 20% hydrogen and the standard deviation of noise as functions of pump power levels. Error bars show the standard deviation from 10 measurements.

IV. Discussions

Our experiments were conducted at room temperature in a lab environment, and no notable influence of temperature on the measured SRS induced dispersion (i.e., dispersion line-shape and magnitude) was observed. However, Raman resonances (i.e. amplitude, resonance frequency and linewidth) are temperature dependent and would affect the characteristics of Raman dispersion when temperature variation becomes large [34], [35]. A full investigation of the effect of temperature on Raman dispersion in gas-filled HC-PCFs should be conducted, particularly for high temperature applications.

In our experiments, gas was pressurized into the HC-PCF through gaps between the HC-PCF and SMF. It took 1-2 hours to achieve uniform distribution of concentration and pressure along the 7-m-long HC-PCF. For practical applications, faster response may be achieved by introducing multiple side -channels along the sensing HC-PCF by use of femtosecond laser micromachining. By drilling multiple micro-channels along a 2.3-m-long HC-PCF, gas filling time as short as ~40s at atmospheric condition has been demonstrated [36].

Currently, the performance of gas detection in terms of NNEC is found mainly limited by the stability of the MZI due to environmental acoustic noise and mode interference noise in the sensing HC-PCF, since the HC-PCF is not a perfect single mode fiber. Acoustic isolation and better high-order mode suppression in the HC-PCF would reduce the system noise level. Once these noises are minimized, other noise sources such as laser fluctuation and modulation instability may need to be assessed in future.

By exploiting Raman induced dispersion, multi-gas detection may be performed. A straightforward configuration for multi-component gas detection may be to use a fixed probe laser and a wavelength-tunable pump laser. The pump wavelength is continuously tuned so that the frequency difference between the probe and the pump is scanned over multiple Raman transitions. With a fixed probe laser, the optical interferometer for phase detection can be fully stabilized, minimizing the effect of environmental noise. Fig. 5 shows the calculated pump wavelengths for the rotational Raman transitions of oxygen, nitrogen and carbon dioxide, assuming that the probe wavelength is fixed to 1550 nm [37]–[39]. A commercial pump laser tunable from 1530 to 1550 nm would allow the detection of the multiple Raman lines of these gases.

V. Conclusions

Laser induced dispersion via SRS in gas-filled optical fibers offers a new way to control the propagation of light with great flexibility. The technique has been demonstrated for hydrogen detection with a normalized noise-equivalent concentration of 17.4 ppm/(m·W) at 3.5 bar and a dynamic range over 4 orders of magnitude. The development of hollow-core fibers with lower loss, broader transmission window and better mode quality [40] as well as the possibility of filling the hollow-core with multiple gases and pumping it with multiple pump sources with flexible wavelengths would enable a range of applications for dynamically controlling light dispersion.

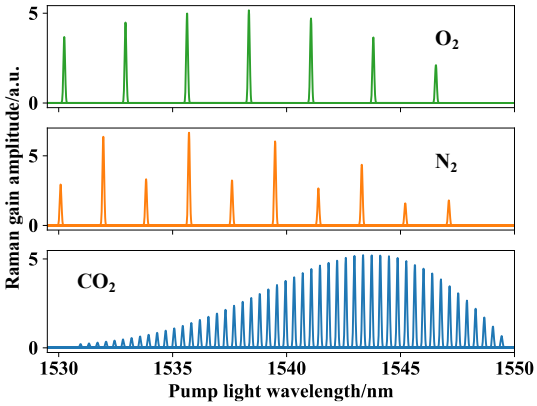

Fig. 5. Calculated rotational Raman transitions of oxygen, nitrogen and carbon dioxide.

Appendix

1. Optimization of modulation depth for 2*f* detection

Wavelength modulation spectroscopy is a popular technique for high sensitivity spectroscopic absorption (gain) measurement [41]. Modulation depth, defined as the ratio of modulation amplitude over the width of absorption (or gain) line, can be optimized to maximize a certain harmonic (e.g. 2*f*) component that is selected to perform the measurement. Similar optimization can be performed for the laser induced dispersion measurement.

Assume that the pump is modulated sinusoidally, the angular frequency of the modulated pump may be expressed as:

$$\omega=\omega_{pump}+\Delta\omega_m \sin(\omega_m t) \ , \qquad \text{(A1)}$$

where $\Delta\omega_m$ is the amplitude and ω_m the frequency of wavelength modulation. Substituting equation (A1) into equation (2), the induced phase modulation of the probe beam may be expressed as:

$$\Delta\phi(t)=\left(\frac{\delta+\delta_m\cos(\omega_m t)}{1+\left(\delta+\delta_m\cos(\omega_m t)\right)^2}\right)\Delta\phi_0 \ , \qquad \text{(A2)}$$

where $\delta_m=2\Delta\omega_m/\Gamma_R$ is the modulation depth. $\Delta\phi(t)$ can be expanded into a series of harmonic signals, and the amplitude of the 2*f* component is [26]:

$$\Delta\phi_2=a_2(\delta,\delta_m)\Delta\phi_0 \ , \qquad \text{(A3)}$$

where $a_2(\delta,\delta_m)$ is an amplitude coefficient. $a_2(\delta,\delta_m)$ as a function of the modulation depth δ_m is plotted as the red solid

line in Fig. A1. The 2*f* signal is maximized at the optimal modulation depth δ_m^{opt} =2.84, giving a_2 = 0.33 [26]. The experimentally measured 2*f* signal using the setup in Fig. 2 is also shown in Fig. A1 as the blue solid dots, which agrees well with the theoretical results.

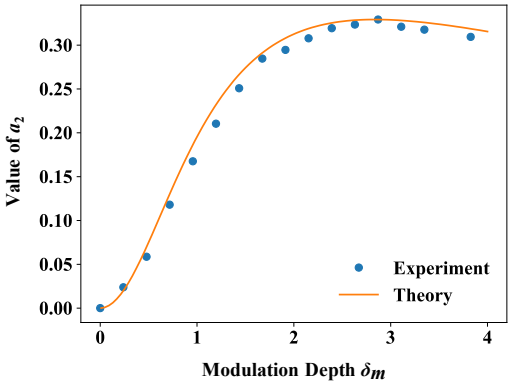

Fig. A1. Amplitude of 2*f*-component of probe phase modulation as a function of modulation depth.

REFERENCES

[1] A. Demircan, S. Amiranashvili, and G. Steinmeyer, "Controlling light by light with an optical event horizon," *Phys. Rev. Lett.*, vol. 106, no. 16, p. 163901, 2011.

[2] G. Rasskazov, A. Ryabtsev, V. V Lozovoy, and M. Dantus, "Laser-induced dispersion control," *Opt. Lett.*, vol. 39, no. 11, pp. 3208–3211, 2014.

[3] N. V Wheeler, P. S. Light, F. Couny, and F. Benabid, "Slow and Superluminal Light Pulses in an Acetylene Filled Photonic Mircocell," *J. Light. Technol.*, vol. 28, no. 6, pp. 870–875, 2010.

[4] S. Ghosh, J. E. Sharping, D. G. Ouzounov, and A. L. Gaeta, "Resonant optical interactions with molecules confined in photonic band-gap fibers," *Phys. Rev. Lett.*, vol. 94, no. 9, pp. 1–4, 2005.

[5] J. Hald, J. C. Petersen, and J. Henningsen, "Saturated optical absorption by slow molecules in hollow-core photonic band-gap fibers," *Phys. Rev. Lett.*, vol. 98, no. 21, pp. 1–4, 2007.

[6] G. Fanjoux and T. Sylvestre, "All-optical tunable pulse frequency chirp via slow light," *Opt. Lett.*, vol. 34, no. 24, pp. 3824–3826, 2009.

[7] L. Thévenaz, "Slow and fast light in optical fibres," *Nat. Photonics*, vol. 2, no. 8, pp. 474–481, 2008.

[8] Y. Okawachi *et al.*, "Tunable all-optical delays via brillouin slow light in an optical fiber," *Phys. Rev. Lett.*, vol. 94, no. 15, pp. 1–4, 2005.

[9] M. González-Herráez, K.-Y. Song, and L. Thévenaz, "Optically controlled slow and fast light in optical fibers using stimulated Brillouin scattering," *Appl. Phys. Lett.*, vol. 87, no. 8, p. 081113, 2005.

[10] A. Lopez-Gil, "Exploiting nonreciprocity in BOTDA systems," *Opt. Lett.*, vol. 40, no. 10, pp. 2193–2196, 2015.

[11] J. B. Khurgin, "Optical buffers based on slow light in electromagnetically induced transparent media and coupled resonator structures: comparative analysis," *J. Opt. Soc. Am. B*, vol. 22, no. 5, p. 1062, 2005.

[12] R. W. Boyd, *Nonlinear optics*. Academic Press, 2008.

[13] J. Bromage, "Raman Amplification for Fiber," *J. Light. Technol.*, vol. 22, no. 1, pp. 79–93, 2004.

[14] M. K. Saxena *et al.*, "Raman optical fiber distributed temperature sensor using wavelet transform based simplified signal processing of Raman backscattered signals," *Opt. Laser Technol.*, vol. 65, pp. 14–24, 2015.

[15] F. Yang and W. Jin, "All-fiber hydrogen sensor based on stimulated Raman gain spectroscopy with a 1550-nm hollow-core fiber," in *Optical Fiber Sensors Conference (OFS), 2017 25th*, 2017, vol. 0, no. 0, p. 103233C.

[16] Y. Han *et al.*, "Index-guiding liquid-core photonic crystal fiber for solution measurement using normal and surface-enhanced Raman scattering," *Opt. Eng.*, vol. 47, no. 4, pp. 040502-1–3, 2008.

[17] G. Agrawal and G. Agrawal, "Chapter 8 – Stimulated Raman Scattering," in *Nonlinear Fiber Optics*, 2013, pp. 295–352.

[18] J. B. Khurgin, R. S. Tucker, and R. S. Tucker, *Slow Light*, vol. 140. CRC Press, 2008.

[19] P. G. Westergaard, M. Lassen, and J. C. Petersen, "Differential high-resolution stimulated CW Raman spectroscopy of hydrogen in a hollow-core fiber," *Opt. Express*, vol. 23, no. 12, pp. 1209–1215, 2015.

[20] F. Benabid, F. Couny, J. C. Knight, and T. A. Birks, "Compact, stable and efficient all-fibre gas cells using hollow-core photonic crystal fibre," *Nature*, vol. 434, no. March, pp. 463–466, 2005.

[21] J. L. Doménech and M. Cueto, "Sensitivity enhancement in high resolution stimulated Raman spectroscopy of gases with hollow-core photonic crystal fibers," *Opt. Lett.*, vol. 38, no. 20, pp. 4074–4077, 2013.

[22] Z. Zhu and D. J. Gauthier, "Numerical study of all-optical slow-light delays via stimulated Brillouin scattering in an optical fiber," *J. Opt. Soc. Am. B*, vol. 22, no. 11, pp. 2378–2384, 2005.

[23] R. G. Wenzel, "Stimulated Rotational Raman Scattering in CO2-Pumped Para-H2," *IEEE J. Quantum Electron.*, vol. QE-19, no. 9, pp. 1407–1413, 1983.

[24] Y. Lin *et al.*, "Pulsed photothermal interferometry for spectroscopic gas detection with hollow-core optical fibre," *Sci. Rep.*, vol. 6, no. 1, p. 39410, Dec. 2016.

[25] W. Jin, Y. Cao, F. Yang, and H. L. Ho, "Ultra-sensitive all-fibre photothermal spectroscopy with large dynamic range," *Nat. Commun.*, vol. 6, 2015.

[26] J. Westberg, P. Kluczynski, S. Lundqvist, and O. Axner, "Analytical expression for the nth Fourier coefficient of a modulated Lorentzian dispersion lineshape function," *J. Quant. Spectrosc. Radiat. Transf.*, vol. 112, no. 9, pp. 1443–1449, 2011.

[27] O. Schmidt, R. Wynands, Z. Hussein, and D. Meschede, "Steep dispersion and group velocity below c/3000 in coherent population trapping," *Phys. Rev. A*, vol. 53, no. 1, pp. R27–R30, 1996.

[28] G. Fanjoux and T. Sylvestre, "Cancellation of Raman pulse walk-off by slow light," *Opt. Lett.*, vol. 33, no. 21, pp. 2506–2508, 2008.

[29] J. Dai *et al.*, "Optical Fiber Grating Hydrogen Sensors: A Review," *Sensors*, vol. 17, no. 3, p. 577, 2017.

[30] G. Korotcenkov, S. Do Han, and J. R. Stetter, "Review of Electrochemical Hydrogen Sensors," *Chemical Review*, vol. 40, no. 22, p. no-no, 2009.

[31] R. Salter, J. Chu, and M. Hippler, "Cavity-enhanced Raman spectroscopy with optical feedback cw diode lasers for gas phase analysis and spectroscopy," *Analyst*, vol. 137, no. 20, pp. 4669–4676, 2012.

[32] S. Hanf, T. Bögözi, R. Keiner, T. Frosch, and J. Popp, "Fast and highly sensitive fiber-enhanced Raman spectroscopic monitoring of molecular H2 and CH4 for point-of-care diagnosis of malabsorption disorders in exhaled human breath," *Anal. Chem.*, vol. 87, no. 2, pp. 982–988, 2015.

[33] M. Nikodem and G. Wysocki, "Molecular dispersion spectroscopy - new capabilities in laser chemical sensing," *Ann. N. Y. Acad. Sci.*, vol. 1260, no. 1, pp. 101–111, 2012.

[34] M. Rokni and A. Flusberg, "Stimulated Rotational Raman Scattering in the Atmosphere," *IEEE J. Quantum Electron.*, vol. 22, no. 7, pp. 1102–1108, 1986.

[35] Herring, G. C., Mark J. Dyer, and W. K. B. "Temperature and density dependence of the linewidths and line shifts of the rotational Raman lines in N2 and H2," *Phys. Rev. A*, vol. 34, no. 3, p. 1944, 1986.

[36] F. Yang, W. Jin, Y. Lin, C. Wang, H. Lut, and Y. Tan, "Hollow-core microstructured optical fiber gas sensors," *J. Light. Technol.*, vol. 35, no. 16, pp. 3413–3424, 2017.

[37] L. C. Hoskins, "Pure rotational Raman spectroscopy of diatomic molecules," *J. Chem. Educ.*, vol. 52, no. 9, p. 568, 1975.

[38] H. Finsterholzl, J. G. Hochenbleicher, and G. Strey, "Intensity Distribution in Pure Rotational Raman-Spectra of Linear-Molecules in Ground and Vibrational 2 States Application To Acetylene," *J. Raman Spectrosc.*, vol. 6, no. 1, pp. 13–19, 1977.

[39] B. L. M. Klarenaar, F. Brehmer, S. Welzel, H. J. van der Meiden, M. C. M. van de Sanden, and R. Engeln, "Note: Rotational Raman scattering on CO_2 plasma using a volume Bragg grating as a notch filter," *Rev. Sci. Instrum.*, vol. 86, no. 4, p. 046106, 2015.

[40] S. Gao *et al*., "Hollow-core conjoined-tube negative-curvature fibre with ultralow loss," *Nat. Commun*., vol. 9, no. 1, p. 2828, 2018.
[41] Schilt, Stephane, L. Thevenaz, and and P. Robert., "Wavelength modulation spectroscopy: combined frequency and intensity laser modulation," *Appl. Opt*., vol. 42, no. 33, pp. 6728–6738, 2003.